JOC Article

Cyclohexanyl Peptide Nucleic Acids (chPNAs) for Preferential RNA Binding: Effective Tuning of Dihedral Angle β in PNAs for DNA/RNA Discrimination

T. Govindaraju, V. Madhuri, Vaijayanti A. Kumar,* and Krishna N. Ganesh*

Division of Organic Chemistry (Synthesis), National Chemical Laboratory, Pune 411008, India

kn.ganesh@ncl.res.in; va.kumar@ncl.res.in

Received June 15, 2005

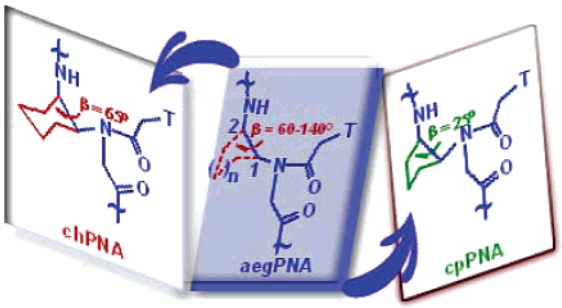

A serious drawback of peptide nucleic acids (PNAs) from an application perspective that has not been adequately dealt with is nondiscrimination of identical DNA and RNA sequences. An analysis of the available X-ray and NMR solution structures of PNA complexes with DNA and RNA suggested that it might be possible to rationally impart DNA/RNA duplex binding selectivity by tuning the dihedral angle β of the flexible ethylenediamine part of the PNA backbone (**II**) via suitable chemical modifications. Cyclohexanyl PNAs (chPNAs) with $\beta \approx 65°$ were designed on the basis of this rationale. The chPNAs introduced remarkable differences in duplex stabilities among their DNA and RNA complexes, with melting temperatures (ΔT_m(RNA−DNA) = +16−50 °C) depending on the number of modifications and the stereochemistry. This is a highly significant, exceptional binding selectivity of a mix sequence of PNA to RNA over the same DNA sequence as that seen to date. In contrast, cyclopentanyl PNAs (cpPNAs) with $\beta \approx 25°$ hybridize to DNA/RNA strongly without discrimination because of the ring puckering of the cyclopentane ring. The high affinity of chPNAs to bind to RNA without losing base specificity will have immediate implications in designing improved PNAs for therapeutic and diagnostic applications.

Introduction

Peptide nucleic acid (PNA, **II**) (Figure 1) is one of the successfully designed oligonucleotide mimics, derived by replacement of the anionic phosphate−sugar backbone with *N*-(1-aminoethyl)glycine units carrying A, G, C, and T nucleobases via methylene carbonyl linkages.[1] Polypyrimidine PNA forms a PNA_2:DNA/RNA triplex, and mixed purine−pyrimidine PNA forms a duplex with a complementary DNA/RNA strand.[2] Because of its high thermal stability and biostability, PNA has great potential for development as an antisense drug[3,4] and also as a probe in affinity-/selectivity-based techniques.[4,5] However, it suffers from major drawbacks such as low cellular uptake, poor aqueous solubility, and equal binding affinity to complementary isosequential DNA/RNA. Further, unlike other DNA mimics, PNA forms hybrids in both parallel (*p*) and antiparallel (*ap*) orientations with complementary nucleic acids. These

* To whom correspondence should be addressed. Fax: 91-20-2589-3153.

(1) Nielsen, P. E.; Egholm, M.; Berg, R. H.; Buchardt, O. *Science* **1991**, *254*, 1497−1501.

(2) (a) Egholm, M.; Buchardt, O.; Christensen, L.; Behrens, C.; Freier, S. M.; Driver, D. A.; Berg, R. H.; Kim, S. K.; Norden, B.; Nielsen, P. E. *Nature* **1993**, *365*, 566−68. (b) Jensen, K. K.; Qrum, H.; Nielsen, P. E.; Norden, B. *Biochemistry* **1997**, *36*, 5072−50.

(3) (a) Uhlmann, E.; Peyman, A.; Breipohl, G.; Will, D. W. *Angew. Chem., Int. Ed.* **1998**, *37*, 2796−2823. (b) Bennett, C. F. In *Applied Antisense Oligonucleotide Technology*; Stein, C. A., Craig, A. M., Eds.; Wiley-Liss. Inc.: New York, 1998. (c) Braasch, D. A.; Corey, D. R. *Biochemistry* **2002**, *41*, 4503−4510.

10.1021/jo051227l CCC: $33.50
Published on Web 12/13/2005

drawbacks have limited the applications of PNA in antisense therapeutics and as a probe for sequence detection. Some of these concerns have been addressed by the introduction of chemical modifications in PNA such as conjugation with transfer ligands including peptides and arbitrary structural modifications of the backbone and side chain.[6−8] The PNAs derived in this way have marginally but unpredictably stabilized or destabilized DNA/RNA hybrids with negligible DNA/RNA or parallel/antiparallel discrimination. The rational strategies of chemical modifications involve the imposition of five- and six-membered heterocyclic rings[8−10] or carbocyclic rings[11] on the aminoethylglycyl (aeg) PNA backbone, with simultaneous introduction of chiral centers. However, these too have not consistently lead to the desired results.

A sufficiently important problem from the application perspective that needs addressing is the nondiscrimination of identical DNA and RNA sequences by PNA antisense molecules with equal affinity to both DNA and RNA, which can access identical sequences but on different targets in the cytoplasm (*m*-RNA) and the nucleus (DNA), leading to undesirable consequences. To address these deficiencies of flexible PNA, we have applied a different rationale for structural design to induce binding selectivity that involves preorganization of the PNA backbone to conformational features attained in PNA:DNA/RNA complexes. A comparison of the currently available X-ray and NMR structural data[12] (Table 1) reveals that the preferred values for the backbone dihedral angle β of a PNA strand in a PNA_2:DNA triplex[13] and a PNA:RNA[14] duplex are in the range 60°−70°, whereas that for a PNA:DNA duplex is about 140°.[15] We construed that the tuning of the dihedral angle β in the flexible ethylenediamine part of the PNA backbone (**II**) through appropriate chemical modifications may lead to preference in DNA/RNA duplex binding. It was previously reported in the literature that 1,2-*trans*-(*R*,*R*/*S*,*S*)-disubstituted cyclohexyl PNA[11a] in an aegPNA backbone destabilized the derived complexes of PNA with both DNA and RNA. It was suggested from molecular modeling studies that the *trans*-cyclohexyl 1,2-substituents occupy the diaxial geometry. This corresponds to a dihedral angle β of ∼180°[11a] which in light of X-ray and NMR data (Table 1) is clearly incompatible with the geometric requirements of either the PNA:DNA or PNA:RNA complexes. Recently, a *trans*-(*S*,*S*)-cyclopentane unit in an aegPNA sequence was shown to marginally stabilize the PNA:DNA complex[11b] and a single *trans*-cyclopropyl-T substituted homothymine aegPNA oligomer was shown to form both a PNA_2:DNA triplex and a PNA:DNA duplex.[11d]

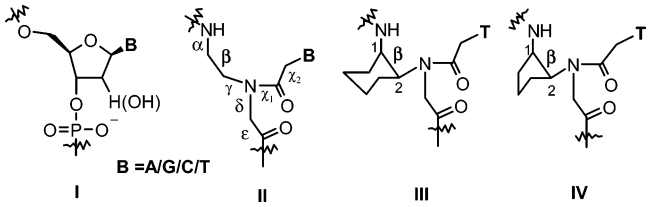

FIGURE 1. Structures of DNA (RNA) **I**, PNA **II**, *cis*-chPNA **III**, and cpPNA **IV**.

In this context, we designed and synthesized the *cis*-1,2 equatorial−axial (*S*,*R*/*R*,*S*)-cyclohexanyl PNA (*cis*-chPNA, **III**), in which the crystal structure of the monomer showed the dihedral angle β of ∼65° and the derived aeg/chPNA chimera formed both PNA_2:DNA and PNA_2:RNA triplexes.[16,17] The substituted cyclohexane ring is inherently rigid and is locked up in either of the two chair conformations. A relatively flexible system would be a cyclopentyl ring,[18] endowed with puckering options. We synthesized *cis*-(*S*,*R*/*R*,*S*)-cyclopentanyl PNA (*cis*-cpPNA, **IV**) monomers in which the dihedral angle β was observed to be ∼25° in the crystal structure.[19] The derived aeg/cpPNA chimeric homo-T oligomers also formed highly stable

(4) (a) Hyrup, B.; Nielsen, P. E. *Bioorg. Med. Chem. Lett.* **1996**, *4*, 5−23. (b) Nielsen, P. E.; Egholm, M. Peptide nucleic acids (PNA). In *Protocols and Applications*; Nielsen, P. E., Egholm, M., Eds.; Horizon scientific press: Norfolk, CT, 1999. (c) Nielsen, P. E. *Curr. Opin. Biotechnol*. **2001**, *12*, 16−20. (d) Nielsen, P. E. *Peptide Nucleic Acids: Methods and Protocols, Methods in Molecular Biology*; Humana Press: Totowa, NJ, 2004; Vol. 208.

(5) (a) Ørum, H.; Nielsen, P. E.; Egholm, M.; Berg, R. H.; Buchardt, O.; Stanley, C. *Nucleic Acid Res*. **1993**, *21*, 5332−5336. (b) Perry-O'Keefe, H.; Yao, X. −W.; Coull, J.; Fuchs, M.; Egholm, M. *Proc. Natl. Acad. Sci. U.S.A.* **1996**, *93*, 14670−14675. (c) Ørum, H.; Nielsen, P. E.; Jørgensen, M.; Larsson, C.; Stanley, C.; Koch, T. *Biotechniques* **1995**, *19*, 472−479. (d) Wang, J.; Palecek, E.; Nielsen, P. E.; Rivas, G.; Cai, X.; Shiraishi, H.; Dontha, N.; Luo, D.; Farias, M. A. *J. Am. Chem. Soc*. **1996**, *118*, 7667−7670.

(6) (a) Ganesh, K. N.; Nielsen, P. E. *Curr. Org. Chem.* **2000**, *4*, 1931−1943. (b) Kumar, V. A.; Ganesh, K. N. *Acc. Chem. Res.* **2005**, *38*, 404−412.

(7) (a) Dueholm, K.; Peterson, K. H.; Jensen, D. K.; Egholm, M.; Nielsen, P. E; Buchardt, O. *Biorg. Med. Chem. Lett.* **1994**, *4*, 1077−1080. (b) Haaima, G.; Lohse, A.; Buchardt, O.; Nielsen, P. E. *Angew. Chem., Int. Ed*. **1996**, *35*, 1939−1942. (c) Puschl, A.; Sforza, S.; Haaima, G.; Dahl, O.; Nielsen, P. E. *Tetrahedron Lett*. **1998**, *39*, 4707−4710. (d) Maison, W.; Schlemminger, I.; Westerhoff, O.; Martens, J. *Bioorg. Med. Chem. Lett.* **1999**, *9*, 581−584. (e) Zhou, P.; Wang, M.; Du, L.; Fisher, G. W.; Waggoner, A.; Ly, D. H. *J. Am. Chem. Soc*. **2003**, *125*, 6878−6879. (f) Hollenstein, M.; Leumann, C. J. *J. Org. Chem*. **2005**, *70*, 3205−3217.

(8) Kumar, V. A. *Eur. J. Org. Chem*. **2002**, 2021−2032.

(9) (a) Gangamani, B. P.; Kumar, V. A.; Ganesh, K. N. *Tetrahedron* **1999**, *55*, 177−192. (b) D'Costa, M.; Kumar, V. A.; Ganesh, K. N. *Org. Lett*. **1999**, *1*, 1513−1516. (c) Vilaivan, T.; Khongdeesameor, C.; Harnyauttanokam, P.; Westwell, M. S.; Lowe, G. *Biorg. Med. Chem. Lett*. **2000**, *10*, 2541−2545. (d) Vilaivan, T.; Khongdeesameor, C.; Harnyauttanokam, P.; Westwell, M. S.; Lowe, G. *Tetrahedron. Lett*. **2001**, *42*, 5533−5536. (e) Hickman, D. T.; King, P. M.; Cooper, M. A.; Slater, J. M.; Micklefield, J. *Chem. Commun*. **2000**, 2251−2252. (f) Puschl, A.; Tedeschi, T.; Nielsen, P. E. *Org. Lett*. **2000**, *2*, 4161−4163. (g) Govindaraju, T.; Kumar, V. A. *Chem. Commun*. **2005**, 495−497.

(10) (a) Puschl, A.; Boesen, T.; Zuccarello, O.; Dahl, O.; Pitsch, S.; Nielsen, P. E. *J. Org. Chem*. **2001**, *66*, 707−712. (b) Lonkar, P. S.; Kumar, V. A. *Bioorg. Med. Chem. Lett*. **2004**, *14/9*, 2147−2149. (c) Shirude, P. S.; Kumar, V. A.; Ganesh, K. N. *Tetrahedron Lett.* **2004**, *45*, 3085−3088. (d) Kumar, V. A.; D'Costa, M.; Lonkar, P. S.; Meena, Pallan, P. S.; Ganesh, K. N. *Pure Appl. Chem*. **2004**, *76*, 1599−1603.

(11) (a) Lagriffoule, P.; Witteng, P.; Ericksson, M.; Jensen, K. K.; Norden, B.; Buchardt, O.; Nielsen, P. E. *Chem.−Eur. J*. **1997**, *3*, 912−919. (b) Myers, M. C.; Witschi, M. A.; Larionova, N. V.; Franck, J. M.; Haynes, R. D.; Hara, T.; Grajkowski, A.; Appella, D. H. *Org. Lett*. **2003**, *5*, 2695−2698. (c) Pokorski, J. K.; Witschi, M. A.; Purnell, B. L.; Appella, D. H. *J. Am. Chem. Soc*. **2004**, *126*, 15067−15073. (d) Pokorski, J. K.; Myers, M. C.; Appella, D. H. *Tetrahedron Lett*. **2005**, *46*, 915−917.

(12) Menchise, V.; Simone, G. D.; Tedeschi, T.; Corradini, R.; Sforza, S.; Marchelli, R.; Capasso, D.; Saviano, M.; Pedone, C. *Proc. Natl. Acad. Sci. U.S.A.* **2003**, *100*, 12021−12026.

(13) Betts, L.; Josey, J. A.; Veal, M.; Jordan, S. R. *Science* **1995**, *270*, 1838−1841.

(14) Brown, S. C.; Thomson, S. A.; Veal, J. M.; Davis, D. J. *Science* **1994**, *265*, 777−780.

(15) Ericksson, M.; Nielsen, P. E. *Nat. Struct. Biol*. **1996**, *3*, 410−413.

(16) Govindaraju, T.; Gonnade, R. G.; Bhadbhade, M. M.; Kumar, V. A.; Ganesh, K. N. *Org. Lett*. **2003**, *5*, 3013−3016.

(17) Govindaraju, T.; Kumar, V. A.; Ganesh, K. N. *J. Org. Chem*. **2004**, *69*, 1858−1865.

(18) Lambert, J. B.; Papay, J. J.; Khan, S. A.; Kappauf, K. A.; Magyar, E. S. *J. Am. Chem. Soc*. **1974**, *96*, 6112−6118.

(19) Govindaraju, T.; Kumar, V. A.; Ganesh, K. N. *Chem. Commun*. **2004**, 860−861.

TABLE 1. Dihedral Angles in ch/cpPNA and PNA in PNA:DNA/RNA Complexes

	PNA_2:DNA[13]	PNA:RNA[14]	PNA:DNA[15]	(1*S*,2*R*)-chPNA[a]	(1*R*,2*S*)-chPNA[a]	(1*S*,2*R*)-cpPNA[a]	(1*R*,2*S*)-cpPNA[a]
α	−103	170	105	128	−129	84	−84
β	73	67	141	−63	66	−24	25
γ	70	79	78	76	−78	86	−86

[a] Values for monomers.[16,19]

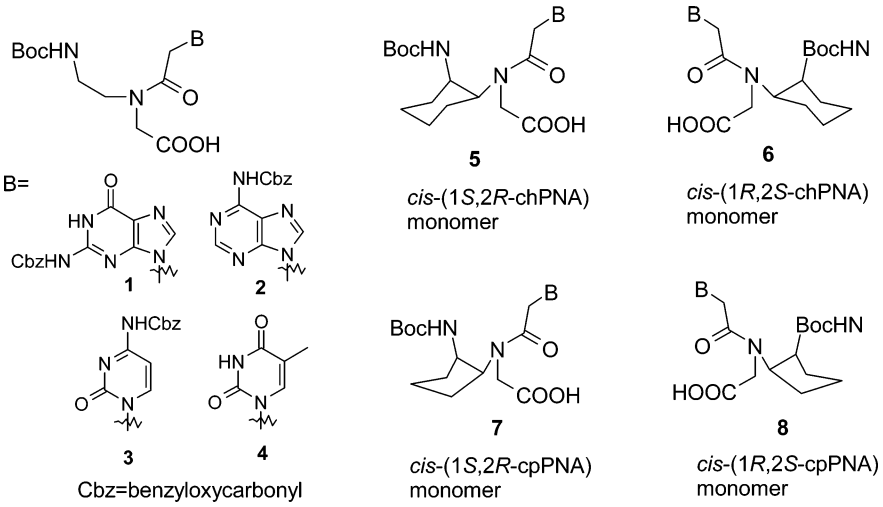

FIGURE 2. Chemical structures of protected monomers of aegPNA (**1**−**4**), chPNA (**5** and **6**), and cpPNA (**7** and **8**).

TABLE 2. RP HPLC and MALDI-TOF Mass Spectral Analysis of Synthesized PNAs

entry	PNA sequences	RT (min)[a]	MF	MW_{calcd}	MW_{obsd}[b]
1	aegPNA **9**, GTAGATCACT-$LysNH_2$	10.50	$C_{114}H_{147}N_{60}O_{31}$	2852.0	2853.0
2	chPNA **10**, GT_{SR}AGAT_{SR}CACT_{SR}-$LysNH_2$	10.64	$C_{126}H_{165}N_{60}O_{31}$	3014.0	3016.0
3	chPNA **11**, GT_{RS}AGAT_{RS}CACT_{RS}-$LysNH_2$	10.71	$C_{126}H_{165}N_{60}O_{31}$	3014.0	3016.0
4	cpPNA **12**, Gt_{SR}AGAt_{SR}CACt_{SR}-$LysNH_2$	9.69	$C_{123}H_{159}N_{60}O_{31}$	2972.0	2974.0
5	cpPNA **13**, Gt_{RS}AGAt_{RS}CACt_{RS}-$LysNH_2$	9.73	$C_{123}H_{159}N_{60}O_{31}$	2972.0	2974.0
6	aegPNA **18**, GGCAGTGCCT-$LysNH_2$	7.99	$C_{113}H_{146}N_{61}O_{32}$	2870.0	2871.1
7	chPNA **19**, GGCAGT_{SR}GCCT-$LysNH_2$	9.10	$C_{117}H_{152}N_{61}O_{32}$	2924.0	2925.5
8	chPNA **20**, GGCAGT_{SR}GCCT_{SR}-$LysNH_2$	10.28	$C_{121}H_{158}N_{61}O_{32}$	2978.0	2979.0
9	chPNA **21**, GGCAGT_{RS}GCCT-$LysNH_2$	9.51	$C_{117}H_{152}N_{61}O_{32}$	2924.0	2925.1
10	chPNA **22**, GGCAGT_{RS}GCCT_{RS}-$LysNH_2$	10.17	$C_{121}H_{158}N_{61}O_{32}$	2978.0	2979.3

[a] RT = retention time (HPLC) in minutes. MF = molecular formula. MW_{calcd} = molecular weight calculated from the corresponding molecular formula. MW_{obsd} = molecular weight observed. [b] Measured on MALDI-TOF spectrometry (for details see Experimental Section). $T_{SR/RS}$ = (1*S*,2*R*)/(1*R*,2*S*)-cyclohexanyl thymine units. $t_{SR/RS}$ = (1*S*,2*R*)/(1*R*,2*S*)-cyclopentanyl thymine units.

PNA:DNA/RNA triplexes without much DNA/RNA discrimination.[19,20]

In this paper, we report the detailed results on DNA/RNA duplex discrimination studies on the mixed-base aeg/chPNA chimera, reported in a recent communication.[21] Significantly, such DNA/RNA discrimination is lacking in aeg/cpPNA analogues. In addition, PNAs **18**−**22**, sequences corresponding to a mutagenic part of the gene that codes for the p53 mutant,[11c] were synthesized with cyclohexanyl-T modifications in both *S*,*R* and *R*,*S* stereochemistries. This strongly validates our design motifs based on the tuning of the dihedral angle *β* to achieve DNA vs RNA selective duplex formation. The synthesis and characterization of aeg/ch/cpPNA oligomers, UV T_m, and circular dichroism (CD) hybridization studies with complementary DNA (*ap*/*p*) and RNA (*ap*/*p*) sequences to detect the DNA/RNA discrimination and *antiparallel* binding preferences are reported. The results have contemporary implications for rational design of PNA modifications for definitive applications.

Results and Discussion

Synthesis of PNA Sequences. All of the four protected aegPNA monomers (Figure 2, **1**−**4**) were synthesized starting from ethylenediamine following the literature procedure.[22] The N-protected enantiomeric *cis*-(1*S*,2*R*)- and *cis*-(1*R*,2*S*)-cyclohexanyl and -cyclopentanyl PNA monomers (Figure 2, **5**−**8**) were synthesized by following the procedures of our earlier reports.[17,20] The unmodified mixed aegPNA decamer **9** (Table 2) was synthesized for use as a control sequence by incorporating the monomers **1**−**4** on MBHA (methyl benzhydrylamine) resin[23] functionalized by L-lysine as a linker to improve the

(20) Govindaraju, T.; Kumar, V. A.; Ganesh, K. N. *J. Org. Chem.* **2004**, *69*, 5725−5734.
(21) Govindaraju, T.; Kumar, V. A.; Ganesh, K. N. *J. Am. Chem. Soc.* **2005**, *127*, 4144−4145.
(22) Dueholm, K. L.; Egholm, M.; Behrens, C.; Christensen, L.; Hansen, H. F.; Vulpius, T.; Petersen, K. H.; Berg, R. H.; Nielsen, P. E.; Buchardt, O. *J. Org. Chem.* **1994**, *59*, 5767−5773.
(23) Matsueda, G. R.; Stewart, J. M. *Peptides* **1981**, *2*, 45−50.

TABLE 3. UV Melting Temperature (°C) of PNA:DNA and PNA:RNA Duplexes[a]

entry	PNA sequences	DNA **14**, *ap* (DNA **16**, *p*)	RNA **15**, *ap* (RNA **17**, *p*)	ΔT_m(RNA−DNA)*ap*
1	aegPNA **9**, GTAGATCACT-LysNH$_2$	55.0[b]	55.4	0.4
2	chPNA **10**, GT_{SR}AGAT_{SR}CACT_{SR}-LysNH$_2$	25.0 (nb)[b]	58.0 (nb)	33
3	chPNA **11**, GT_{RS}AGAT_{RS}CACT_{RS}-LysNH$_2$	35.0 (nb)[b]	>85.0 (80)	>50
4	cpPNA **12**, Gt_{SR}AGAt_{SR}CACt_{SR}-LysNH$_2$	77.1 (nb)	84.0 (71)	6.9
5	cpPNA **13**, Gt_{RS}AGAt_{RS}CACt_{RS}-LysNH$_2$	78.8 (71)	>85.0 (84)	>6.2

[a] All values are an average of at least three experiments and are accurate to within ±0.5 °C. Buffer. Sodium phosphate (10 mM), pH 7.0 with 100 mM NaCl and 0.1 mM EDTA. [b] Measured by CD to avoid interference from thermal transitions of single-stranded PNAs.[11a] A, T, G, and C are aegPNA bases. $T_{SR/RS}$ = *cis*-cyclohexanyl-T units (**10** and **11**). $t_{SR/RS}$ = *cis*-cyclopentanyl-T units (**12** and **13**). DNA **14**, 5′-AGTGATCTAC-3′ (*ap*); RNA **15**, 5′-AGUGAUCUAC-3′ (*ap*); DNA **16**, 5′-CATCTAGTGA-3′(*p*); RNA **17**, 5′-CAUCUAGUGA-3′ (*p*). Values in brackets are T_m of parallel duplexes. nb = no binding.

solubility of the PNA oligomers.[24] The resin with an initial loading value of 0.25 meq/g and the reagents HBTU [2-(1*H*-benzotriazole-1-yl)-1,1,3,3-tetramethyluronum hexafluorophosphate], HOBt (1-hydroxybenzotriazole), and DIEA (diisopropylethylamine) in DMF/DMSO were used in the coupling step. The *cis*-cyclohexanyl (**5** and **6**) and *cis*-cyclopentanyl (**7** and **8**) thymine monomers were incorporated into aegPNA oligomer **9** at three thymine positions by standard solid-phase synthesis protocols on MBHA resin optimized in our earlier studies (**10**−**13**, Table 2).[17,20] The PNAs were cleaved from the resin with TFA−TFMSA (trifluoromethane sulfonic acid),[25] followed by purification using reverse-phase high-performance liquid chromatography (RP HPLC) to yield the oligomers **9**−**13** in more than 90% purity and characterization by MALDI-TOF mass spectral data (Table 2).

All the PNAs synthesized were found to have good water solubility, despite the presence of hydrophobic *cis*-cyclohexanyl and *cis*-cyclopentanyl units, due to the presence of L-lysine. The purity of DNA/RNA after desalting was ascertained to be >99% by RP HPLC, and DNA/RNA was used without further purification for all hybridization studies (for details, see Experimental section). The 10-mer PNA sequences **10**−**13** belong to the same sequence as the control **9** but with cyclohexanyl-T (*T*) or cyclopentanyl-T (*t*) modifications corresponding to *S*,*R* and *R*,*S* confugurations at identical sites. In addition, PNAs **18**−**22**, corresponding to a sequence with the potential for p53 antisense repression,[11c] and an 18-mer PNA **27** were synthesized with cyclohexanyl-T modifications, with both *S*,*R* and *R*,*S* stereochemistries. The complementary deoxyribooligonucleotides (DNA) designed to bind complementary PNAs in both parallel and antiparallel modes (**14**, **16**, **23**, and **28**−**33**) were synthesized on an automated parallel DNA synthesizer,[26] and ribooligonucleotides (RNA; **15**, **17**, and **24**) were procured from commercial sources, and 18-mer RNA sequences **33** and **34** were a kind gift from Dr. M. Manoharan.

UV Thermal Melting Studies of PNA:DNA/RNA Duplexes. The T_m values of different PNAs hybridized with cDNA/RNA for parallel and antiparallel binding were determined from temperature-dependent UV absorbance or CD plots and are summarized in Table 3. It is seen from the UV melting temperature data (Table 3) obtained from the melting curves (for UV T_m/CD T_m curves, see Supporting Information) that the control aegPNA **9** (entry 1) formed *ap* duplexes with complementary DNA **14** and RNA **15** with almost equal stability. In comparison, the T_m values of chPNA:DNA duplexes (entries 2 and 3) are considerably lower (ΔT_m = −30 °C for *S*,*R* and −20 °C for *R*,*S*). The thermal stability of chPNA duplexes with a complementary DNA oligonucleotide was stereochemistry dependent, with the T_m of the *R*,*S* duplex being higher than that of the *S*,*R* duplex (ΔT_m = 10−30 °C for chPNA). chPNAs **10** and **11** having low binding affinity with *antiparallel* DNA **14** were ineffective in forming parallel duplexes with complementary DNA **16**. In the case of PNA/RNA duplexes, the (*R*,*S*)-chPNA **11** (entry 3) had a large stabilizing effect, having a T_m value >85 °C (ΔT_m > 30 °C) higher than that of the control aegPNA/RNA duplex, whereas the corresponding parallel duplex (**11:17**) showed complete melting, with a lower T_m (Supporting Information). The (*S*,*R*)-chPNA/RNA antiparallel duplex (**10:15**) (entry 2) having a T_m of 58 °C was only marginally stabilized (ΔT_m = 2.6 °C). The most important feature of the data in Table 2 is that (*S*,*R*/*R*,*S*)-chPNAs form highly stable duplexes with complementary RNA as compared to their duplexes with complementary DNA. Thus, (*S*,*R*/*R*,*S*)-*cis*-chPNAs designed on the dihedral angle considerations induced remarkable differences in duplex stabilities between their complexes with DNA and RNA, with ΔT_m(RNA−DNA) being +33 °C for *S*,*R*-chPNA **10** and +50 °C for *R*,*S*-chPNA **11**. This is a very significant, exceptional binding selectivity of a modified PNA to RNA over the same DNA sequence.

The thermal stability measurements of the duplexes (Table 3) formed by (*S*,*R*)-cpPNA **12** (entry 4) and (*R*,*S*)-cpPNA **13** (entry 5) with antiparallel complementary DNA **14** (Table 3, entries 4 and 5, respectively) indicated a large increase in the T_m (ΔT_m = +22 °C and +24 °C, respectively) compared to that of the aegPNA/DNA duplex (entry 1). The (*R*,*S*)-cpPNA:DNA (**13:14**) duplex is marginally more stable than the (*S*,*R*)-cpPNA:DNA (**12:14**) duplex (ΔT_m = +2 °C) (Table 3). The modified mixed backbones of (*S*,*R*/*R*,*S*)-cpPNAs (**12** and **13**) also showed a higher stability of their corresponding duplexes with antiparallel complementary RNA **15** (ΔT_m = +27 °C for (*S*,*R*)-cpPNA **12**; ΔT_m > +27 °C for (*R*,*S*)-cpPNA **13**) compared to the corresponding complexes of unmodified aegPNA **9**. However, the stability differences between the cpPNA/DNA and cpPNA/RNA duplexes were much smaller (ΔT_m = +6 °C for *S*,*R*-cpPNA **12**; ΔT_m > +6 °C for *R*,*S*-cpPNA **13**), with RNA duplexes being more stable than DNA duplexes. The (*R*,*S*)-cpPNA:RNA (**13:15**) transition, which is >85 °C, was not detected in the temperature range 5−85 °C and was indirectly confirmed by a decreased T_m observed for the parallel duplex

(24) Egholm, M.; Buchardt, O.; Nielsen, P. E. *J. Am. Chem. Soc*. **1992**, *114*, 1895−1897.

(25) Christensen, L.; Fitzpatrick, R.; Gildea, B.; Petersen, K. H.; Hansen, H. F.; Koch, T.; Egholm, M.; Buchardt, O.; Nielsen, P. E.; Coull, J.; Berg, R. H. *J. Pept. Sci*. **1995**, *3*, 175.

(26) (a) Gait, J. M. *Oligonucleotides: A practical approach*; IRL Press: Oxford, U.K., 1984; 217. (b) Agarval, S Protocols for oligonucleotides and Analogues: Synthesis and properties. In *Methods in Molecular Biology*; Agaraval, S., Ed.; Humana Press Inc.: Totowa, NJ, 1993; Vol. 20.

TABLE 4. UV Melting Temperature (°C) Values of PNA:DNA and PNA:RNA Duplexes[a]

entry	PNA sequence (p53)	DNA **23**, *ap*	RNA **24**, *ap* (RNA **26**, *p*)	ΔT_m(RNA−DNA)*ap*
1	aegPNA **18**, GGCAGTGCCT-LysNH$_2$	59.5	64.0 (59.5)	4.5
2	*S*,*R*-chPNA **19**, GGCAGT_{SR}GCCT-LysNH$_2$	58.5	74.5	16.0
3	*S*,*R*-chPNA **20**, GGCAGT_{SR}GCCT_{SR}-LysNH$_2$	55.5	>85.0 (80.0)	>30.0
4	*R*,*S*-chPNA **21**, GGCAGT_{RS}GCCT-LysNH$_2$	57.0	83.0	26.0
5	*R*,*S*-chPNA **22**, GGCAGT_{RS}GCCT_{RS}-LysNH$_2$	56.0	>85.0 (∼84.0)	>30.0

[a] All values are an average of at least three experiments and are accurate to within ±0.5 °C. Buffer: sodium phosphate (10 mM), pH 7.0, with 100 mM NaCl and 0.1 mM EDTA. A, T, G, and C are aegPNA bases. $T_{SR/RS}$ = *cis*-cyclohexanyl-T unit (**19**−**22**). DNA **23**, 5′-AGGCACTGCC-3′ (*ap*); RNA **24**, 5′-AGGCACUGCC-3′ (*ap*); DNA **25** (parallel) = 5′-CCGTCACGGA-3′; RNA **26** (parallel) = 5′-CCGUCACGGA-3′. Values in brackets are T_m for parallel PNA:DNA and PNA:RNA duplexes.

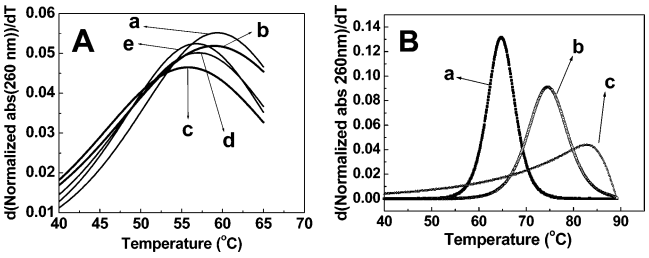

FIGURE 3. UV T_m curves for **A**: **PNA:DNA** antiparallel duplexes of (a) aegPNA **18**, (b) *S*,*R*-chPNA **19**, (c) *S*,*R*-chPNA **20**, (d) *R*,*S*-chPNA **21**, and (e) *R*,*S*-chPNA **22** with DNA **23**. **B**: UV T_m derivative curves for **PNA:RNA** antiparallel duplexes of (a) aegPNA **18**, (b) *S*,*R*-chPNA **19**, and (c) *S*,*R*-chPNA **21** with RNA **24**. DNA **23** (antiparallel) = 5′-AGGCACTGCC-3′. RNA **24** (antiparallel) = 5′-AGGCACUGCC-3′. Buffer = 10 mM sodium phosphate buffer, pH = 7, 100 mM, NaCl, 0.1 mM EDTA.

13:17 (entry 5, value in brackets). The (*R*,*S*)-cpPNA **13** also showed a lower affinity to form a parallel duplex with DNA **16** (ΔT_m < 8 °C), and the proper melting transition could not be assigned for (*S*,*R*)-cpPNA:DNA (**12:16**) complex.

To establish the validity of RNA selectivity effects observed for chPNAs **10** and **11**, a biologically relevant[11c] aegPNA sequence (**18**) was synthesized. This PNA sequence is complementary to a portion of the gene that encodes the mutant p53 protein found in many different cancer cell lines.[27] chPNAs **19**−**22** were synthesized by incorporating *S*,*R*/*R*,*S*-*cis*-cyclohexanyl-T monomers at either one (Table 4, **19** and **21**) or both (Table 4, **20** and **22**) thymine positions. The T_m data obtained from thermal melting curves (Figure 3) are shown in Table 4. As compared to the DNA/RNA complexes of unmodified aegPNA **18**, the chPNAs **19**−**22** marginally destabilized the duplexes with corresponding antiparallel complementary DNA **23**, and the duplexes with *ap* RNA **24** were highly stabilized. The chPNAs **19** and **20** (Table 4, entries 2 and 3) stabilized duplexes with RNA **24** (*S*,*R*-chPNA **19**, ΔT_m = +10 °C; *S*,*R*-chPNA **20**, ΔT_m = +20 °C) and destabilized the hybrids with DNA **23** (*S*,*R*-chPNA **19**, ΔT_m = −1 °C; *S*,*R*-chPNA **20**, ΔT_m = − 4 °C). The results were more pronounced in the case of *R*,*S*-chPNA. Even a single substitution of *R*,*S*-chPNA-T in a decamer of chPNA **21** showed a 19 °C increase in T_m compared to that of aegPNA **18** (Table 4, entries 4 and 5). The ΔT_m(RNA−DNA) of +26° C (entry 4) with double substitution (entry 5, chPNA **22**) makes the chPNA:RNA hybrid more stable with a ΔT_m-(RNA−DNA) greater than 30 °C. Increasing the number of substitutions from one (cpPNA:DNA **21:23**, ΔT_m = −2 °C) to two (cpPNA:DNA **22:23**, ΔT_m = −3 °C) also destabilized the corresponding DNA hybrids. As observed for the chPNA sequence **11**, the *R*,*S* isomer is better than the *S*,*R* isomer in achieving discrimination.

The chPNAs **19**−**22** bind DNA in an antiparallel orientation but do not form hybrids with parallel DNA **25**. chPNAs **19** and **21** with a single modification bind RNA only in the antiparallel mode and not in the parallel mode, whereas the PNAs **20** and **22** with two modified units form parallel PNA:RNA hybrids with a T_m marginally lower than that for the antiparallel hybrids. The combined UV T_m data from Tables 3 and 4 also suggest that the increased thermal stability (T_m) of the chPNA:RNA duplex is uniformly consistent, irrespective of the position of the modified *cis*-cyclohexanyl-T units. The *S*,*R*/*R*,*S*-chPNAs showed a rise in the T_m of ≥10 °C per ch-T unit in the sequence, and the effect seems to be additive with multiple ch-T units.

UV T_m Studies on Mismatched Duplexes. To see the effect of mismatches on cpPNA:DNA/RNA duplexes, a representative 18-mer cpPNA **27** having three cpPNA-T modifications was chosen. This was hybridized with complementary antiparallel DNA **28**, parallel DNA **29**, and parallel RNA **33** to generate corresponding cpPNA:DNA/RNA duplexes. Additionally, cpPNA:DNA antiparallel duplexes with three T:T mismatches (**27:31**), one T:C mismatch (**27:32**), and three T:C mismatches (**27:33**), all having a mismatched site opposite to the cpPNA sites, were also studied for thermal stability. Similarly, the cpPNA:RNA parallel duplex **27:34** represented a typical case for an RNA mismatch. The melting profiles are shown in the Supporting Information, and the derived UV T_m values are shown in Table 5.

The results in Table 5 indicate that cpPNA **27** binds to complementary DNA and RNA almost equally well (entries 1, 2, and 6) but with marginal stability for *ap*DNA **28** compared to *p*DNA **29**. The cpPNA **27** also bound to parallel RNA **33** better than parallel DNA **29**. Introduction of three T mismatches in DNA **30** opposite to the cpPNA substitutions destabilized the duplexes by more than 25 °C (Table 5, entry 3). A single C mismatch, as in DNA **31**, destabilized the duplexes much more (ΔT_m > 55 °C), and DNA **32** with three C mismatches did not bind cpPNA **27** (Table 5, entries 4 and 5). This is a consequence of the relative-stability tolerence of T:T and T:C mismatches. Compared to these results on DNA, T:C mismatch-induced destabilization was not significant in the case of RNA **34** (Table 5, entries 6 and 7). Further work is needed to establish the stereochemistry and base-dependent destabilization effects of mismatches in ch- and cpPNAs.

Circular Dichroism (CD) Studies of PNA:DNA/RNA Duplexes. The two enantiomeric chPNA monomers (**5** and **6**) showed mirror image CD spectra (Supporting Information). The

(27) (a) Hollstein, M.; Rice, K.; Greenblatt, M. S.; Soussi, T.; Fuchs, R.; Sorlie, T.; Hovig, E.; Smith-Sorenson, B.; Montesano, R.; Harris, C. C. *Nucleic Acid Res.* **1994**, *22*, 3551−3555. (b) Hainaut, P.; Soussi, T.; Shomer, B.; Hollstain, M.; Greenblatt, M.; Hovig, E.; Harris, C. C.; Montesano, R. *Nucleic Acid Res*. **1997**, *25*, 151−157.

TABLE 5. UV Melting Temperature (T_m) in °C of cpPNA 27:DNA:RNA Duplexes[a]

entry	DNA/RNA	T_m
1	DNA **28**, 5′-TGT AAC TGA GGT AAG AGG-3′ (*ap*)	>85
2	DNA **29**, 5′-GGA GAA TGG AGT CAA TGT-3′ (*p*)	73
3	DNA **30**, 5′-TGT TAC TGT GGT ATG AGG-3′ (*ap*)	60
4	DNA **31**, 5′- TGT $\overline{\text{A}}$AC T$\overline{\text{G}}\overline{\text{C}}$ GGT $\overline{\text{A}}$AG AGG-3′ (*ap*)	30.2
5	DNA **32**, 5′- TGT $\underline{\text{C}}$AC T$\underline{\text{G}}\overline{\text{C}}$ GGT A$\underline{\text{C}}$G AGG-3′ (*ap*)	nb
6	RNA **33**, 5′-GGA $\overline{\text{G}}$AA U$\overline{\text{G}}\overline{\text{G}}$ AGU C$\overline{\text{A}}$A UGU-3′ (*p*)	>85
7	RNA **34**, 5′-GGA GAA U$\underline{\text{G}}\underline{\text{C}}$ AGU CAA UGU-3′ (*p*)	~85

[a] cpPNA **27** H−CCT C*t*T ACC *t*CA GT*t* ACA-LysNH$_2$ (*t* = 1*R*,2S-cpPNA). T/C in DNA **30**, **31**, **32**, and RNA **34** indicates the sites mismatched to cpPNA **27**. Buffer: 10 mM phosphate (pH 7.4) and 10 mM NaCl. [PNA] = 0.5 μM. $\overline{\text{A}}$ll T_m values are an average of three independent experiments and are accurate to within ±0.5 °C.

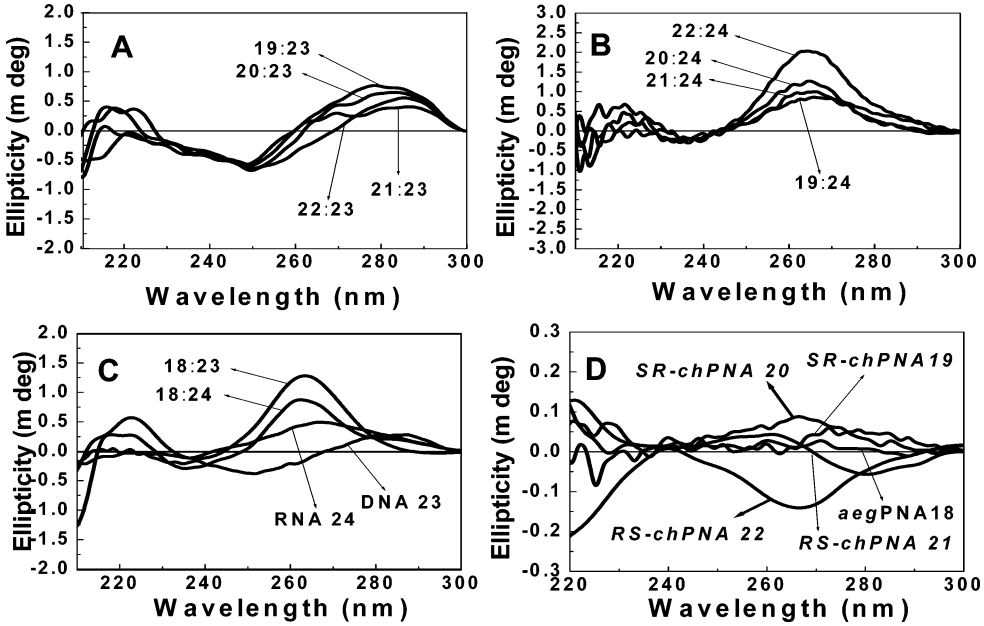

FIGURE 4. CD spectra of PNA:DNA/RNA duplexes of **A**: chPNA:DNA duplexes (a) **19:23**, (b) **20:23**, (c) **21:23**, and (d) **22:23**. **B**: chPNA:RNA duplexes (a) **19:24**, (b) **20:24**, (c) **21:24**, and (d) **22:24**. **C**: aegPNA:DNA/RNA duplexes (a) **18:23**, (b) **18:24**, and (d) ssDNA **23**, and (e) ssRNA **24**. **D**: CD spectra of single-stranded (ss) chPNAs (a) **19**, (b) **20**, (c) **21**, and (d) **22**. (10 mM sodium phosphate buffer, pH = 7, 100 mM, NaCl, 0.1 mM EDTA.)

single-stranded PNAs containing chiral (1*S*,2*R*)- and (1*R*,2*S*)-aminocyclohexanyl or -cyclopentanyl modifications exhibited weak but distinct CD spectra. The single-stranded chPNA **10**/**11** and cpPNA **12**/**13** pairs also showed near mirror image CD spectra. The CD spectra are not exactly related, as mirror images are expected for enantiomeric pairs due to the presence of L-lysine at the C-terminus of PNA sequences. Because of the dominant CD contributions from DNA/RNA strands in the complexes, the differences due to *S*,*R*/*R*,*S* isomeric modifications are not apparent in the CD spectra of ch/cpPNA:DNA/RNA hybrids.

The (*S*,*R*/*R*,*S*)-ch/cpPNA:DNA (**10:14**, **11:14**) and (*S*,*R*/*R*,*S*)-cpPNA:DNA (**12:14**, **13:14**) duplexes showed CD profiles (Supporting Information) similar to that of the aegPNA/DNA (**9**/**14**) duplex,[28] with a positive band at 277 nm and a low intensity negative band at 250 nm. The CD profiles of (*S*,*R*/*R*,*S*)-chPNA:RNA (**10:15**, **11:15**) and (*S*,*R*/*R*,*S*)-cpPNA:RNA duplexes consisted of a high intensity positive band (260−270 nm) and a low intensity negative band (245 nm) similar to that of the aegPNA/RNA (**9:15**) duplex, suggesting a high degree of helical identity among the aeg/ch/cp-PNA:RNA duplexes. The CD features of cpPNA:DNA duplexes (**12**/**13:14**) are akin to their RNA duplexes (**12**/**13:15**) implying that cpPNA:DNA duplexes can adopt a more RNA-like structure with higher stability. The larger elliptic intensities seen in cpPNA:RNA duplexes are indicative of a better base stacking in these compared to cpPNA:DNA duplexes.

The CD spectra of chPNA (**19**−**22**):DNA:RNA duplexes were found to have more interesting structural features, which support the RNA selectivity observed from the corresponding UV T_m measurements. These chPNA:DNA duplexes show CD with a maximum intensity band at 280 nm and a minimum intensity band at 250 nm (Figure 4A). These are similar to the CD of single-stranded DNA **23** but with slightly enhanced intensity and a different appearance from that of the aegPNA:DNA (**18**:**23**) duplex (Figure 4C). This perhaps suggests that the chPNA:DNA duplexes inherently form less-ordered structures. In contrast, RNA duplexes derived from chPNAs (**19**−**22**) show CD profiles (Figure 4B) similar to that of the aegPNA:RNA (**18:24**) duplex (Figure 4C) with enhanced intensity, indicating the formation of well-structured A-type duplexes. The intensity of the CD profiles depends on the number and stereochemistry of *cis*-cyclohexanyl-T modifications in the PNA sequences. chPNAs **20** and **22** with two modified cyclohexa-

(28) Kim, S. K.; Nielsen, P. E.; Egholm, M.; Buchardt, O.; Berg, R. H. *J. Am. Chem. Soc.* **1993**, *115*, 6477−6483.

nyl-T units show higher intensity CD signatures (Figure 4B, b and d) when compared to chPNAs **19** and **21** with a single modified unit (Figure 4C, b and d). This arises from enhanced base stacking and supports the additive behavior of increased T_m of PNA:DNA/RNA hybrids seen in thermal UV transitions.

The CD signatures of single-stranded chPNAs (**19**−**22**) show weak signals (Figure 3D). The CD profiles of chPNAs with *S*,*R* and *R*,*S* stereochemistry are nearly mirror images, and one cyclohexanyl-T unit (Figure 4D, *S*,*R*-chPNA **19** and *R*,*S*-chPNA **21**) even introduced chirality to the aegPNA **1** inducing a characteristic CD in aegPNA chimera. The effect of cyclohexanyl-T units was additive as seen by the enhancement in the CD intensity of chPNAs **20** and **22** (Figure 4D) with two cyclohexanyl-T units compared to that of chPNAs **19** and **21** with single modification accompanied by a slight shift of the bands.

Discussion

Classical aegPNA, being conformationally flexible, can easily attain a competent conformation to hybridize with DNA and RNA equally well, as seen by near equal PNA:DNA/RNA duplex T_m. In (*S*,*R*/*R*,*S*)-chPNA, the monomer dihedral angle β matches the range (65°) found in the PNA/RNA duplex rather than that in the PNA:DNA duplex (140°). The derived chPNAs thus exhibit a higher affinity to RNA and destabilize the complex with DNA. (*S*,*R*/*R*,*S*)-cpPNA with a lower dihedral angle β (25°) binds to both RNA and DNA with a higher avidity compared to aegPNA and chPNA but lacks the differentiating ability of chPNA. This binding preference seen in duplexes is somewhat reverse of that in triplexes derived from homothymine PNAs.[17,20] The T_m results also suggest that both ch- and cpPNAs, irrespective of their stereochemistry, prefer the antiparallel mode of binding to complementary oligonucleotides. In the five-membered rings of cpPNA and DNA, the flexible ring puckering allows better torsional adjustments to mutually compatible hybridization-competent conformations. On the other hand, the inherently rigid six-membered ring of chPNAs, being locked up in either of the two conformations, forbids structural adjustments as in cpPNA. Further, in ch/cpPNAs, the favorable conformational features of the monomer seem to be cooperatively transmitted to the oligomer level even in a mixed aeg/ch/cpPNA backbone. The observed dihedral angle β (25°) in the cpPNA crystal structure is not suitable for either PNA:RNA (∼65°) or PNA:DNA (140°) complex formation and seems to readjust in solution in the presence of complementary DNA/RNA sequences. The cpPNA allows the readjustment of the ring puckers via pseudorotation of the flexible five-membered ring, and hence, cooperative interaction is observed with both DNA and RNA. The observed dihedral angle of 65° for β in the (*S*,*R*/*R*,*S*)-chPNA crystal structure matches the dihedral angle seen for the PNA strand in PNA:RNA duplexes, and the resultant entropic gain from preorganization imparts an unparalleled selectivity for binding to RNA. The rigidity of the cyclohexyl ring disfavors its readjustment to the structurally compatible DNA geometry necessary for PNA:DNA duplexes ($\beta = 140°$), and therefore, complexes with DNA are much less stable (<16−50 °C).

The rationale of the present work on the design of preorganized backbones and the results are in accordance with many biochemical recognitions mediated by the steric/induced fit model.[29] As a general property, the cis geometry of both cyclohexane and cyclopentane rings has a very profound effect on the binding affinities of chPNA and cpPNA to complementary DNA or RNA compared to the corresponding trans analogues.[11] The *trans*-cyclohexyl PNA, with inappropriate geometry and inherent cyclohexyl rigidity, fails to elicit binding to complementary DNA/RNA. It should be pointed out that, unlike the cyclohexanyl rings, there is not much difference in the dihedral angle between cis and trans isomers in the cyclopentanyl system. The puckering flexibility may perhaps be the reason for the reported *trans*-cyclopentyl PNA and also stabilizes duplexes with DNA, though marginally compared to the strong stabilization by *cis*-cyclopentyl PNA demonstrated here; the corresponding RNA binding data for *trans*-cpPNA are not available for making an effective comparison with the present *cis*-cpPNA.

To rationalize the observed remarkable preference for RNA binding, it is tempting to ask to what extent the incorporation of a single modification affects the overall conformation of the oligomer. It has been observed that the presence of a single ribose sugar at the terminus of a 10-mer deoxyoligonucleotide chain is enough to force A-conformation for the DNA duplex, instead of the preferred B-form.[30] Thus, the hybridization-competent, rigid conformation of a single chPNA monomer is able to transmit its features along the unmodified chain, to sustain a favorable conformation for preferential RNA recognition. Though we are yet to make homooligomers of the present modifications, deductions drawn here on the effect of five- vs six-membered rings in the PNA backbone have somewhat parallel analogies with the pioneering studies reported on six-membered hexose[31] and carbocyclic nucleic acids.[32]

Conclusion

We have demonstrated that the conformationally constrained *cis*-cyclohexanyl-T monomer-incorporated PNAs (**10**, **11**, and **19**−**22**) show an unprecedented preference to form a duplex with RNA as compared with DNA. The *cis*-cyclopentanyl PNA analogues (**12** and **13**) bind remarkably well with both complementary DNA and RNA strands but lack a DNA/RNA discriminating property. The observed differences in DNA/RNA affinity between *cis*-cyclohexanyl and *cis*-cyclopentanyl PNAs arise from differences in their relative backbone flexibility. The rigidity of the *cis*-cyclohexane ring results in a fixed dihedral angle, $\beta \sim 65°$, appropriate for RNA selectivity, whereas the flexible *cis*-cyclopentane ring with a reduced angle, $\beta \sim 25°$, is prone to adapt for complementation with both DNA and RNA. Such higher binding of cyclopentanyl PNAs to both DNA and RNA is a consequence of the ease of conformational adjustments in a cyclopentane ring through ring puckering in contrast to the rigid locked chair conformations of a cyclohexane system. Delineating the relative contributions of these properties may help to achieve optimal fine tuning of PNA chemical modifications to attain balanced affinity/selectivity toward target sequences.

(29) Demidov, V. V.; Frank-Kamenetskii, M. D. *Trends Biochem. Sci.* **2004**, *29*, 62−71.
(30) Ban, C.; Ramakrishnan, B.; Sundaralingam, M. *Nucleic Acid Res.* **1994**, *22*, 5466−5476.
(31) Schöning, K.-U.; Scholz, P.; Guntha, S.; Wu, X.; Krishnamurthy, R.; Eschenmoser, A. *Science* **2000**, *290*, 1347.
(32) Lescrinier, E.; Froeyen, M.; Herdewijn, P. *Nucleic Acid Res.* **2003**, *31*, 2975−2989.

The present results showcasing the strong preference of (*S,R*/*R,S*)-chPNA to bind RNA are in consonance with our strategy of adjusting dihedral angle β through chemical modifications to achieve structure-based selectivity in PNAs. The modification or conjugation of PNAs with cell penetrating ligands may also prompt their nuclear entry. The induction of binding selectivity for DNA/RNA complements would be therefore desirable to improve the efficiency of nucleic-acid-based drugs.[33] The presence of carbocyclic structures may also facilitate PNA cellular uptake due to hydrophobic interaction with the lipid bilayer. Further studies aimed at delineation of PNA's promiscuous RNA/DNA binding on a structure-based rationale, base (T/A/G/C) sequence dependence of carbocyclic modifications, and efficiency of cellular uptake are in progress.

Experimental Section

Synthesis of PNA Oligomers Incorporating *cis*-(1*S*,2*R*)- and (1*R*,2*S*)-Aminocyclohexanyl (Pentanyl) PNA Monomers. The control aegPNAs **9** and **18** were synthesized using a standard procedure on a L-lysine derivatized (4-methyl benzhydryl)amine (MBHA) resin (initial loading of 0.25 meq g^{-1}) with HBTU/HOBt/DIEA in DMF/DMSO as a coupling reagent. The *S,R/R,S*-ch/cpPNA monomers were built into aegPNA oligomers **9** and **18** at predefined thymine positions. The manual synthesis using 4.0 equiv of the monomers and coupling reagents with respect to the resin loading value and a coupling time of 2.5−3.0 h are found to be optimum. The PNA oligomers were cleaved from the resin with TFMSA. The oligomers were purified by RP HPLC (C18 column) and characterized by MALDI-TOF mass spectrometry. The overall yields of the raw products were 50−75%.

Cleavage of the PNA Oligomers from the Resin. The MBHA resin (20 mg) with the attached PNA oligomer was stirred with thioanisole (40 μL) and 1,2-ethanedithiol (32 μL) in an ice bath for 10 min. TFA (240 μL) was added, and after equilibrium for 10 min, TFMSA (32 μL) was added slowly. The reaction mixture was stirred for 2.5 h at room temperature, filtered, and concentrated under vacuum. The product was precipitated with dry ether from methanol, and the precipitate was dissolved in water (200 μL) and loaded over a Sephadex G25 column. Fractions of 0.5 mL were collected, and the presence of an oligomer was detected by measuring the absorbance at 260 nm. The fractions containing oligomers were freeze-dried, and the purity of the fractions was assessed by analytical RP HPLC. If the purity was less than 90%, oligomers were purified by preparative HPLC.

Gel Filtration. The crude PNA oligomer obtained after ether precipitation was dissolved in water (200 μL) and loaded onto a gel filtration column. This column consisted of G25 Sephadex and had a void volume of 1.0 mL. The oligomer was eluted with water, and 10 fractions of 0.5 mL volume each were collected. The presence of the PNA oligomer was detected by measuring the absorbance at 260 nm. The fractions containing the oligomer were freeze-dried. The purity of the cleaved crude PNA oligomer was determined by RP HPLC on a C18 column. If the purity of the oligomers was found to be above 96%, the oligomers were used as such for experiments without further purification; otherwise, the oligomers were purified by HPLC. The oligomers were found to be stable for a long time when stored at −20 °C as dry solids. In solution, the crude PNAs were stable up to a week and were found to undergo polymerization to give insoluble precipitate on keeping for a long duration.

HPLC (High Performance Liquid Chromatography) Purification of PNA Oligomers. The crude PNAs were purified on a semipreparative C18 column attached to a Hewlett-Packard 1050 HPLC system equipped with an auto sampler and a variable-wavelength detector. A gradient elution method contained A = 0.1% trifluoromethane sulfonic acid in water and B = 50% CH_3CN in water (A to B = 50% in 30 min with a flow rate of 1.5 mL/min), and the eluent was monitored at 260 nm. The purity of the oligomers was further assessed by an RP-C18 analytical HPLC column (25 × 0.2 cm; 5 mm) with gradient elution (A to B = 50% in 20 min, A = 0.1% TFA in H_2O, B = 0.1% TFA in CH_3CN/H_2O 1:1 with a flow rate of 1 mL/min). The purities of the purified oligomers were found to be >98%.

MALDI-TOF Mass Spectrometry. The purity and integrity of the PNAs synthesized in this study were ascertained by HPLC and later confirmed by MALDI-TOF (matrix assisted laser desorption ionization time-of-flight) mass spectrometry in which several matrices have been explored, viz., sinapinic acid (3,5-dimethoxy-4-hydroxycinnamic acid), CHCA (α-cyano-4-hydroxycinnamic acid), and DHB (2,5-dihydroxybenzoic acid). With ch/cpPNAs, sinapinic acid was found to give the best signal-to-noise ratio of all the other matrixes typically producing higher molecular ion signals. For all the MALDI-TOF spectra recorded for the PNAs reported, sinapinic acid was used as the matrix and was found to give satisfactory results.

UV T_m Measurements. The concentrations of PNAs were calculated on the basis of absorbance from the molar extinction coefficients of the corresponding nucleobases (i.e., T, 8.8 cm^2/μmol; C, 7.3 cm^2/μmol; G, 11.7 cm^2/μmol, and A, 15.4 cm^2/μmol). The complexes were prepared in 10 mM sodium phosphate buffer, pH 7.0, containing NaCl (100 mM) and EDTA (0.1 mM) and were annealed by keeping the samples at 85 °C for 5 min followed by slow cooling to room temperature (annealing). Absorbance versus temperature profiles were obtained by monitoring at 260 nm with a UV−vis spectrophotometer scanning from 5 to 85/90 °C at a ramp rate of 0.2 °C per minute. The data were processed using Microcal Origin 5.0 and T_m values derived from the derivative curves.

Circular Dichroism. CD spectra were recorded on a spectropolarimeter. The CD spectra of the PNA:DNA/RNA complexes and the relevant single strands were recorded in 10 mM sodium phosphate buffer (100 mM, NaCl, 0.1 mM EDTA, pH 7.0). The temperature of the circulating water was kept below the melting temperature of the PNA:DNA/RNA complexes, i.e., at 10 °C. The CD spectra of the mixed-base PNAs and the derived PNA:DNA/RNA duplexes were recorded as an accumulation of 10 scans from 320 to 195 nm using a 1 cm cell, a resolution of 0.1 nm, a bandwidth of 1.0 nm, sensitivity of 2 mdeg, a response of 2 s, and a scan speed of 50 nm/min.

Synthesis of Complementary Oligonucleotides. The DNA oligonucleotides used in the PNA:DNA hybridization studies were synthesized on a high throughput DNA synthesizer using standard β-cyanoethyl phosphoramidite chemistry. The oligomers were synthesized in the 3′ to 5′ direction on a polystyrene solid support, followed by ammonia treatment. The oligonucleotides were desalted by gel filtration and their purity was ascertained by RP HPLC on an analytical C18 column to be more than 98%; they were used without further purification in the biophysical studies of PNAs. The corresponding cRNA oligonucleotides were obtained commercially.

Acknowledgment. T.G. thanks CSIR, New Delhi, for the award of a Research Fellowship. We acknowledge IFCPAR, New Delhi, for partial financial assistance for the project. K.N.G. is also a Senior Honorary Professor at Jawaharlal Nehru Centre for Advanced Scientific Research, Bangalore. We thank Anita Gunjal for assistance in DNA synthesis.

Supporting Information Available: Synthesis details, HPLC profiles, MALDI-TOF mass spectra of ch/cpPNAs, UV T_m, and CD curves. This material is available free of charge via the Internet at http://pubs.acs.org.

JO051227L

(33) (a) Hunziker, J. *Chimia* **2001**, *55*, 1038−1041. (b) Liu, Y.; Braasch, D. A.; Corey, D. R. *Biochemistry* **2004**, *43*, 1921−1927.